The Ocular Surface 37 (2025) 236–246

Contents lists available at ScienceDirect

The Ocular Surface

journal homepage: www.elsevier.com/locate/jtos

High Impact Original Research

Dessicating stress triggers and exacerbates experimental ocular Graft-versus-host-disease☆

Uta Gehlsen [a,1], Martina Maass [a,1], Daniela Stary [a], Svenja Wagener-Ryczek [b], Gwen Musial [a], Manolis Pasparakis [c], Cintia S. de Paiva [d], Michael E. Stern [a], Philipp Steven [a,*]

[a] Competence Center for Ocular GVHD, Center of Integrated Oncology, Department I of Internal Medicine and Department of Ophthalmology, Faculty of Medicine and University Hospital Cologne, Germany
[b] Institute of Pathology, University of Cologne, Faculty of Medicine and University Hospital Cologne, Germany
[c] Institute for Genetics, Cologne Excellence Cluster on Cellular Stress Responses in Aging-Associated Diseases (CECAD) and Center for Molecular Medicine (CMMC), University of Cologne, Cologne, Germany
[d] Ocular Surface Center at the Cullen Eye Institute, Department of Ophthalmology, Baylor College of Medicine, Houston, TX, USA

ARTICLE INFO

Keywords:
Ocular graft-versus-host disease
Desiccating stress
Allogeneic hematopoietic stem cell transplantation
Risk factor

ABSTRACT

Introduction: Chronic ocular graft-versus-host disease (oGVHD) is one of the most common complications after allogeneic hematopoietic stem cell transplantation (aHSCT). Recent studies indicate that desiccating stress by air-conditioning in transplantation wards increases the incidence of oGVHD. To test the hypothesis that experimental desiccating stress is a risk factor for oGVHD a mouse model of oGVHD was subjected to experimental desiccating stress.

Materials/Methods: A previously established chemo-induced minor-mismatch mouse model of oGVHD was used. One group was challenged with desiccating stress for 18 days and compared to non-desiccated GVHD animals. Clinical phenotyping was performed weekly and ocular tissue and regional lymph nodes were collected on days 7 and 28 for flow-cytometry, tear film cytokine analysis, histology for corneal lymphatics and dendritic cell counts, and corneal gene expression.

Results: Desiccating stress leads to significant earlier and more severe systemic and oGVHD accompanied by higher numbers of activated corneal dendritic cells, higher expression of TNF in tear film and earlier corneal lymphangiogenesis. Gene expression analysis suggests that systemic GVHD severity may influence oGVHD. Different inflammatory pathways are upregulated at d28 following desiccating stress in contrast to non-desiccated GVHD.

Conclusions: The data presented strengthens the hypothesis, that desiccating stress during aHSCT is a risk factor for oGVHD. Together with already published clinical data, there is increasing evidence that implicates protecting patients from desiccation during the engraftment of allogeneic hematopoietic stem cells. Furthermore, specific prophylactic therapies should be developed and tested to reduce the incidence and severity of oGVHD.

1. Introduction

Chronic ocular graft-versus-host disease (oGVHD) is one of the most common complications after allogeneic hematopoietic stem cell transplantation (aHSCT). Up to 60 % of patients develop this severe, often rapidly progressive disease [1,2]. Clinically, the ocular surface is usually affected, especially the eyelids, conjunctiva, cornea, and lacrimal gland. However, in rare cases, the retina is also involved [3]. Although the clinical phenotype resembles dry eye, oGVHD should be viewed as a separate entity due to its specific pathomechanisms and treated accordingly.

The general pathogenesis of graft-versus-host disease (GVHD) is divided into 3 phases [4]. In the first phase, inflammation of the tissue including activation of damage- and pathogen-associated molecular

☆ Presented in part at these meetings: Association for Research in Vision and Ophthalmology 2021, International Ocular Surface Society 2022, International Expert Meeting on ocular GVHD 2024.

* Corresponding author.
E-mail address: philipp.steven@uk-koeln.de (P. Steven).

[1] These authors contributed equally.

https://doi.org/10.1016/j.jtos.2025.04.008
Received 6 February 2025; Received in revised form 10 April 2025; Accepted 13 April 2025
Available online 24 April 2025

patterns as well as antigen-presenting cells (APCs) and platelets, occurs during tumor therapy and subsequent conditioning [5]. In the second phase, donor B and T cells are activated, and alloreactive cells are expanded [6]. These alloreactive cells migrate to the periphery, leading to inflammation and damage of target organs such as skin, mucosa, and solid organs. Furthermore, damage to the thymus leads to a reduction in regulatory B and T cells and a loss of peripheral tolerance [7]. In the third phase, chronic macrophage activation leads to fibroblast activation and consecutive formation of extracellular matrix with fibrosis of tissues [8].

A comparable pathogenesis is assumed for oGVHD. Preclinical and clinical studies have proven the activation of APCs, tissue damage by alloreactive T cells, and fibrosis of the conjunctiva and lacrimal gland, and anti-inflammatory and regenerative therapies have been developed based on this concept [9]. However, except for topical cyclosporine, these therapeutic measures have not been tested before or at the onset of oGVHD [10–12].

In contrast to most other ocular diseases, chronic oGVHD is in principle predictable, as it always follows a previous aHSCT. Thus, it seems ideally suited for therapeutic avoidance. However, suitable prediction models and reliable prophylactic measures have yet to be established. This would require the identification of reliable risk factors for the development of chronic oGHVD and a detailed understanding of the early pathomechanisms, particularly phases 1 and 2 of GVHD pathogenesis, as discussed above.

Recently, our group has shown by clinical retrospective studies that desiccating stress of <30 % humidity with constant airflow during aHSCT leads to oGVHD in more than 70 % of cases. In contrast, oGVHD occurs in only 30 % of cases when humidity is >50 % during transplantation [13,14]. These studies indicate that desiccating stress, which occurs primarily in winter in our hospital, may be a risk factor for developing oGVHD. Prophylactic avoidance of the same or raising the humidity to >50 % could thus reduce subsequent chronic oGVHD. An alternative pathway could be a specific therapeutic intervention of the pathomechanisms.

To understand the role of ocular surface desiccation in the pathogenesis of oGVHD and, in particular, to analyze early immune mechanisms, mouse animal models of oGVHD [15–22] and dry eye produced by experimental desiccating stress [23,24] are suitable. In this study, we combined both models and investigated early immune mechanisms in the development of oGVHD to test the hypothesis that experimental desiccation stress is a risk factor for the development of oGVHD.

2. Material and methods

2.1. Animal model and clinical in vivo readouts

GVHD was induced as described in detail previously [22,25]. Briefly, female C57BL/6 (H2k^b) recipient mice received a chemotherapy conditioning protocol using busulfan and cyclophosphamide monohydrate (both Sigma-Aldrich, Germany) followed by allogeneic transplantation of bone marrow cells and splenic T cells from a 129S2/SvPasCrl (H2k^b) donor (both strains Charles River Laboratories; Sulzfeld, Germany). Blood samples were analyzed by flow cytometry using Ly9.1 and H2kb as chimerism markers at the end of the experiments to ensure successful engraftment. After the transplantation mice were examined once a week for clinical parameters of systemic GVHD (weight loss, posture, activity, fur, and skin abnormalities) on a scale from 0 to 2 for each parameter and oGVHD. Ocular parameters (blepharitis, tear production, corneal epitheliopathy) were investigated at baseline and 7, 14, 21, and 28 days after transplantation as described in detail previously [22,24]. To quantify blepharitis (lid swelling, loss of fur around the eyes scored from 0-(no swelling or loss of fur) to 2-(severe swelling, loss of fur as described in Ref. [22]) and corneal damage (fluorescein staining grade scored from 0 to 5), images were taken and analyzed by two blinded observers (UG and MM). Clinical characteristics of the eyes seen in this model resemble typical features of chronic ocular GVHD in humans in contrast to acute oGVHD features such as chemosis and pseudomembranes [22].

To investigate the effect of adverse environmental conditions on oGVHD mice were exposed to desiccating stress (DS) with reduced humidity (<30 % RH) and a constant airflow (GVHD-DS) from day 1–18 after transplantation and compared with GVHD mice (GVHD) that were housed under standard conditions (>50 % RH, no airflow). Since it is known, that desiccating stress itself can induce ocular surface disease [26–28], a further control group of naïve mice exposed to DS but without GVHD was used in some experiments.

All experiments were performed at least two times with n = 5 mice per group. At baseline and on days 7 and 28 after transplantation, mice were sacrificed and cornea, conjunctiva, and draining lymph nodes were excised. Tissue samples of naïve C57BL/6 mice were used as a control.

All experiments were performed in agreement with ARRIVE guidelines and according to the EU Directive 2010/63/EU for animal experiments and the Landesamt für Natur, Umwelt und Verbraucherschutz (LANUV) of the state of Nordrhein-Westfalia (license number A388).

2.2. Dendritic cell and vessel quantification in the cornea

Corneal flat-mount tissue samples were fixed in acetone, blocked with 2 % bovine serum albumin in PBS, and incubated (1:100) overnight with anti-LYVE1, FITC-labeled CD31, and AlexaFluor™647-labeled CD11c antibodies (for detailed information of antibodies used see supplemental table). Whole-mount RGB images were then semi-automatically analyzed using a custom program (MATLAB, The MathWorks, Inc., Natick, MA) and a custom built-in Python algorithm to calculate the area of the cornea covered by lymphatics or blood vessels as described previously [22]. The number of CD11c + dendritic cells was counted manually using the free software ImageJ. Each final image was analyzed in a blinded manner by one experienced observer.

2.3. Flow cytometry

Single-cell suspensions from cervical lymph nodes were prepared by meshing the tissue through a 40 µl cell strainer and lysing the erythrocytes with Hybrid-Max™ lysing buffer (Sigma Aldrich). The pellet was re-suspended in FACS buffer (2 % fetal bovine serum, 0.2 % HEPES in Dulbeccos PBS). Cells were blocked with anti-mouse CD16/CD32 FC-block (BD Pharmingen, clone 2.4G2) and incubated with either anti-CD4, CD8, CD25, FoxP3, or anti-CD11c, MHC II, CD40, CD80, CD86 antibodies according to the manufacturer's instructions (for detailed information of antibodies and reagents used see supplemental table). After incubation, cells were re-suspended in serum-free PBS and incubated with eBioscience™fixable viability dye eFluor™ 450 (Invitrogen). Cells were washed and fixed with BD™ Stabilizing fixative (BD Bioscience) 1:3 in *aqua dest.* Measurements were executed using a BD FACSCanto™II cell analyzer (BD Biosciences). Data was analyzed using FlowJo software (FlowJo LLC, OR, US).

2.4. Tear film cytokine analysis

For tear film analysis, 2 µl of PBS was applied without contact on the central corneal surface, and the mouse was allowed to blink. Tear washings were then carefully collected with a 2 µl glass capillary from the lateral canthus of the eye. Tear samples were stored at −80 °C until further processing. For the detection of cytokines (IFN-γ, IL-2, IL-4, IL-6, IL-10, TNF) a LUNARIS™ Mouse 6-Plex Cytokine Kit (Ayoxxa, Cologne, Germany) was used according to the manufacturer's instructions. Samples were diluted 1:2 with the assay diluent and loaded onto the biochip together with the provided protein standards. After labeling the analytes with streptavidin-phycoerythrin, the biochip was dried overnight at room temperature and measured using a LUNARIS™ Reader™ 96/384. For data analysis, the LUNARIS™ Analysis Suite (Ayoxxa) was

used.

2.5. Gene expression and pathway analysis

Total RNA was extracted from conjunctival and whole corneal tissue from one eye from GVHD and GVHD-DS mice using the Qiagen RNeasy Plus Mini kit with a genomic DNA eliminator spin column according to the manufacturer's instructions. RNA was diluted in RNase-free water and the concentration, as well as the purity, were determined using a spectrophotometer device (NanoDrop, Thermo Fisher). To analyze the gene expression a commercial oligonucleotide microarray technology (NanoString nCounter® Autoimmune Profiling Panel, NanoString Technologies, Seattle, WA, US) was used as described in detail in the literature [29] and according to the manufacturer's instructions. 250 ng of each RNA sample (n = 3 samples per group) were hybridized to capture probes each carrying a unique, target-specific, color code. Target/probe complexes were imaged using a nCounter Digital Analyzer (NCT-DIGA-120, NanoString Technologies) and analyzed using the ROSALIND (Onramp, San Diego, CA, US). Pathway analyses were investigated using metascape (metascape.org).

2.6. Statistics

Data were analyzed using either the non-parametric Friedmann test for paired samples (repeated measures of each group over time) with the Bonferroni corrected Dunn's post-hoc-test or, depending on the sample number, the Kruskal-Wallis-test or Mann-Whitney-U-test for unpaired samples was used to compare differences between GVHD and GVHD-DS. A p-value below 0.05 was considered statistically significant by convention. SPSS (v.25) was used for statistical analysis. Data is

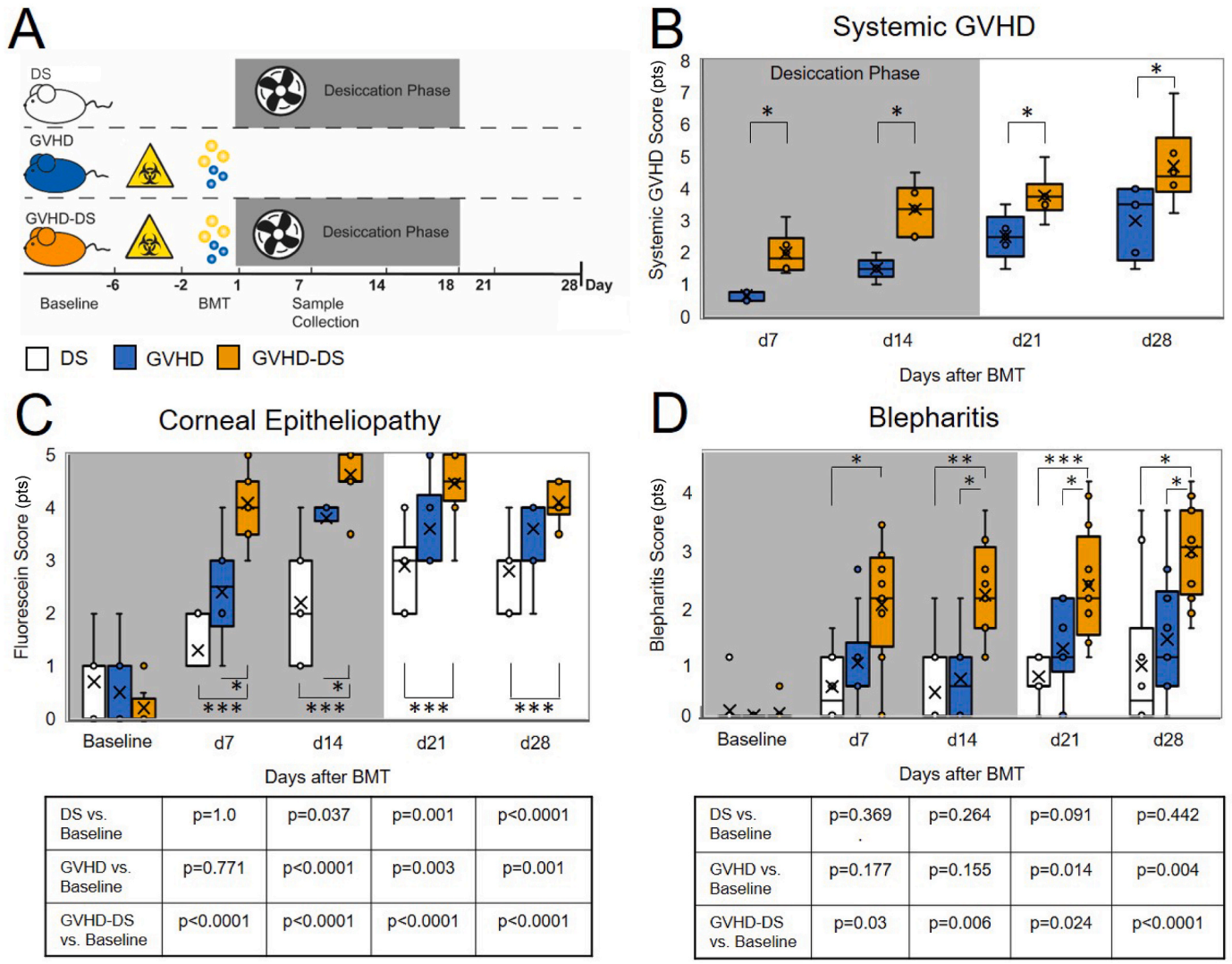

DS vs. Baseline	p=1.0	p=0.037	p=0.001	p<0.0001
GVHD vs. Baseline	p=0.771	p<0.0001	p=0.003	p=0.001
GVHD-DS vs. Baseline	p<0.0001	p<0.0001	p<0.0001	p<0.0001

DS vs. Baseline	p=0.369	p=0.264	p=0.091	p=0.442
GVHD vs. Baseline	p=0.177	p=0.155	p=0.014	p=0.004
GVHD-DS vs. Baseline	p=0.03	p=0.006	p=0.024	p<0.0001

Fig. 1. Experimental set-up and clinical in vivo GVHD readouts. A) Mice received allogeneic transplantation of bone marrow and T cells (BMT) after 4 days of chemotherapy to induce GVHD. One experimental group was exposed to desiccating stress after BMT until d18 (GVHD-DS), in the control group GVHD was induced without DS (GVHD). A further control group of healthy mice without GVHD was also exposed to DS (DS). **B)** In the GVHD-DS group the systemic GVHD score was significantly increased from d7 ($p = 0.007$) after BMT compared to GVHD mice. Mice at baseline and naïve-DS do not develop a GVHD score and were therefore not included in the graph. **C)** Time course of corneal epithelial damages from baseline until day 28 after BMT. The GVHD-DS group developed a significantly earlier and more severe fluorescein staining at d7 compared to GVHD ($p = 0.012$) and naïve-DS ($p = 0.0001$). In the GVHD and naïve-DS control, the onset of fluorescein staining occurred one week later at d14 after BMT. **D)** Time course of blepharitis from baseline until d28 after BMT. The lid margin inflammation started significantly earlier in GVHD-DS and was increased compared to baseline ($p = 0.03$) and naïve-DS ($p = 0.05$) at day 7. In GVHD control mice blepharitis started at d21 after BMT and remained significantly lower compared to GVHD-DS. ($n = 5$ mice/group; *$p \leq 0.05$, **$p \leq 0.001$, ***$p \leq 0.0001$. Asterisks directly below/above boxplots refer to comparison with DS-control mice. Comparison between GVHD-DS and GVHD is indicated by brackets. BMT = bone marrow transplantation, DS = desiccation stress, d = day, X = mean, line in box = median, whiskers = upper (maximum number) and lower (minimum number) quartiles).

presented as a boxplot graph, with the box showing the median (line) and 1st to 3rd quartile and the whiskers showing the upper (maximum number) and lower (minimum number) quartiles of the data set. Within the box, the mean is visualized as X.

3. Results

3.1. Desiccating stress after BMT exacerbates signs of systemic and ocular GVHD

To investigate the potential pathogenic role of desiccation on the development of oGVHD, mice were subjected to our BMT transplant protocol with and without desiccation. Naïve C57BL/6 mice were used as positive controls for dry eye induction (Fig. 1A). GVHD-DS mice demonstrated a significantly higher systemic GVHD score from d7 until d28 after BMT compared to non-desiccated GVHD mice. In GVHD-DS the systemic score increased already from d7 to d14 from 2.0 ± 0.6 to 3.4 ± 0.8 ($p = 0.045$), whereas in the GVHD-only group, the systemic score increased the earliest at d21 (2.5 ± 0.7). The difference between both groups at d7 was highly significant (0.7 ± 0.1) ($p = 0.007$). The systemic GVHD score remained at a higher level in the GVHD-DS group (d21: 3.8 ± 0.7; d28: 4.7 ± 1.3) even after the end of the desiccation compared to GVHD (d21: 2.5 ± 0.7; d28: 3.0 ± 1.2) (d21: $p = 0.009$); d28: $p = 0.03$) (Fig. 1B).

Ocular GVHD phenotype was assessed using corneal fluorescein and the blepharitis score. At d7 after BMT the corneal fluorescein score was already significantly increased in GVHD-DS (4.1 ± 0.6) compared to baseline (0.2 ± 0.4; $p < 0.0001$), DS only control (0.7 ± 0.7; $p < 0.0001$), and GVHD without DS (2.4 ± 1.0; $p = 0.012$) (Fig. 1 C). At d14 the fluorescein score increased also in DS (2.2 ± 1.0; $p = 0.037$) and GVHD (3.8 ± 0.4; $p < 0.0001$) and remained at an increased level compared to baseline, but was still significantly lower compared to GVHD-DS (4.6 ± 0.4)(DS: $p < 0.0001$; GVHD: $p = 0.026$). GVHD mice reached a comparable level of fluorescein as GVHD-DS mice not before d21 ($p = 0.09$) (Fig. 1 C).

Blepharitis increased at d7 after BMT in GVHD-DS (1.9 ± 1.1; p =

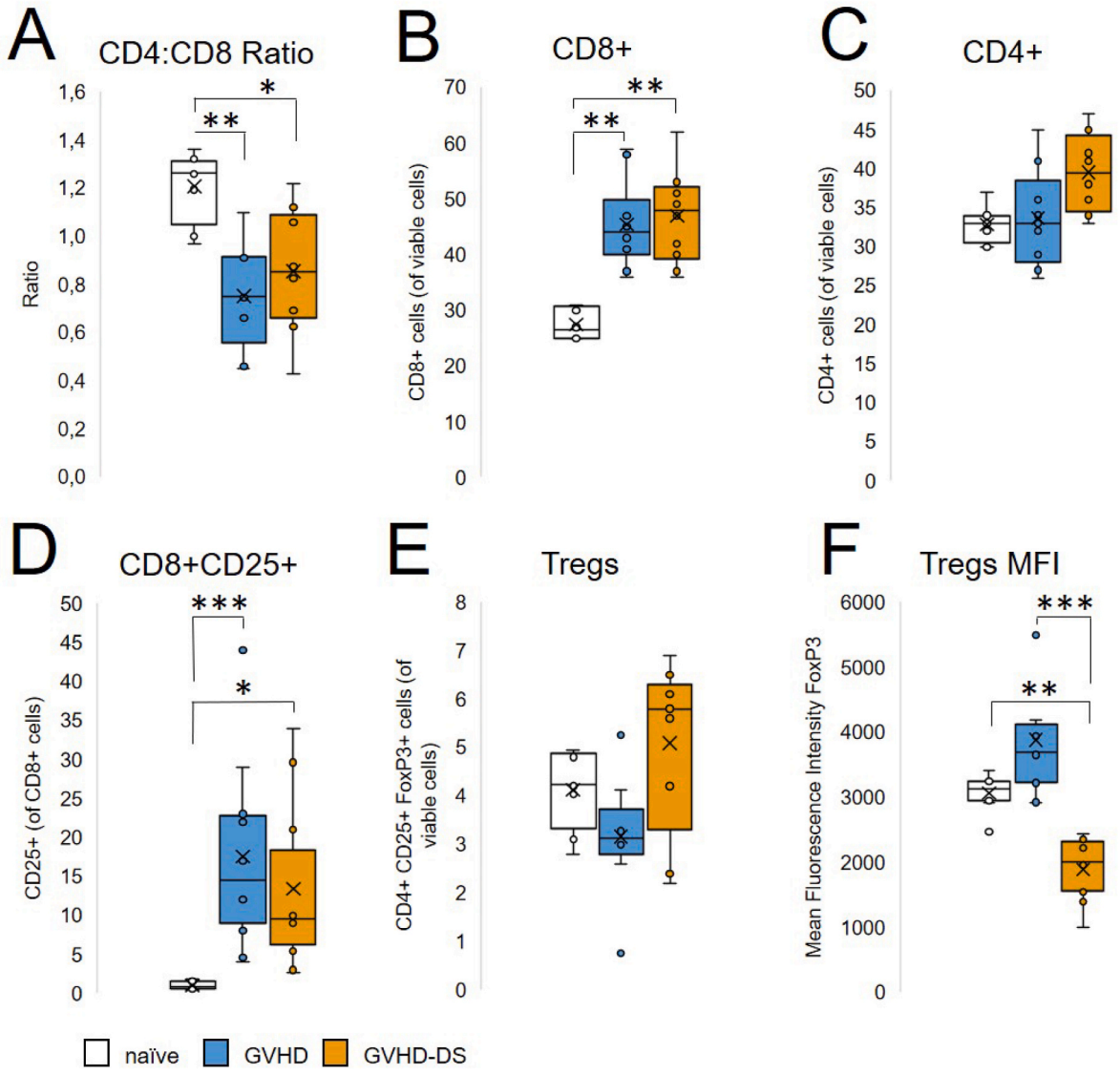

Fig. 2. T Cell analysis in cervical lymph nodes in GVHD-DS and GVHD mice at day 7 after BMT. A) The CD4:CD8 ratio was decreased in both GVHD ($p = 0.001$) and GVHD-DS ($p = 0.01$) mice compared to naïve mice. **B)** The frequency of $CD8^+$ cells was increased in GVHD ($p = 0.001$) and GVHD-DS ($p = 0.01$) compared to naïve mice. **C)** The frequency of $CD4^+$ T cells was not changed. **D)** In GVHD ($p = 0.0001$) and GVHD-DS ($p = 0.003$) a significantly higher number of $CD8^+$ cells were $CD25^+$. **E + F)** The frequency of FoxP3+ regulatory T Cells was not changed in any group, but the mean fluorescence intensity of FoxP3 was significantly decreased in GVHD-DS compared to naïve ($p = 0.01$) and GVHD ($p = 0.0001$) mice indicating a reduced frequency of these cells. ($n = 5–8$ mice/group; *$p \leq 0.05$, **$p \leq 0.001$, ***$p \leq 0.0001$. Treg-regulatory T Cell, MFI-mean fluorescence intensity).

0.03) compared to baseline but remained at a baseline level in naïve-DS (0.5 ± 0.6) and GVHD (0.9 ± 0.8) until d21 (Fig. 1 D). At d21 the blepharitis score was also increased in GVHD (1.2 ± 0.7; p = 0.014) compared to baseline but was significantly lower than in the GVHD-DS (2.2 ± 1.0; p = 0.05) even after the end of desiccating stress (Fig. 1 D). Because of the early significant differences between GVHD and GVHD-DS groups, the following analyses were focused on d7 after BMT.

These results indicate that desiccation after BMT worsens the clinical parameters of oGVHD.

3.2. Increase of $CD8^+$ T cells and DC-activation and early loss of treg-functionality in cervical lymph nodes

Expansion and activation of T-cells and dysfunction of Tregs have been described in the pathology of ocular GVHD [17,18,30].

CD4:CD8 ratio in the cervical lymph nodes was significantly decreased in both GVHD and GVHD-DS mice (0.7 ± 0.2; 0.8 ± 0.3) compared to naïve mice (1.2 ± 0.1)(GVHD: p = 0.001, GVHD-DS: p = 0.011) after 7 days, due to an increase of $CD8^+$ T cells (45 ± 8 %; 47 ± 8 %; naïve: 27 ± 3 %) (Fig. 2A and B). The number of $CD4^+$ T cells remained stable at early stages (p = 0.270) (Fig. 2 C). A significantly higher number of $CD8^+$ T cells expressed the activation marker CD25 in both of the GVHD groups (18 ± 12 %, 13 ± 11 %) compared to $CD8^+$ T cells from naïve controls (1 ± 1 %)(GVHD: p ≤ 0.0001; GVHD-DS: p = 0.003) (Fig. 2 D). The frequency of regulatory T cells (Tregs, measured as $CD4^+CD25^+FoxP3^+$) was between 3 and 5 % and did not change at d7 after BMT in GVHD, GVHD-DS, and naïve controls (p = 0.061). However, the level of FoxP3 depicted by the mean fluorescence intensity (MFI) was significantly reduced in GVHD-DS compared to GVHD (p ≤ 0.0001) and non-desiccated (p = 0.010) groups.

Dendritic cell activation is a hallmark of oGVHD [31]. We hypothesized that desiccation would increase the frequency of mature APCs. Therefore, ocular draining lymph nodes were collected, and levels of CD40, CD80, and CD86 were investigated. Furthermore, the number of mature (MHC II^+CD11c^+) dendritic cells (DC) was increased in both GVHD (12 ± 4 %) and GVHD-DS (23 ± 10 %) compared to naïve (6 ± 3 %)(GVHD: p = 0.038; GVHD-DS: p ≤ 0.0001), but significantly higher in GVHD-DS compared to GVHD (p = 0.018) at d7 after BMT (Fig. 3 A). In the GVHD-DS group, DCs expressed significantly more activation markers (CD40: p = 0.006; CD80: p = 0.02; and CD86: p = 0.045) than GVHD. In contrast, the activation state of DCs in the GVHD group was not changed at d7 compared to DCs from naïve controls (CD40: p = 0.785; CD80: p = 0.063; CD86: 0.136) (Fig. 3B–E).

3.3. Early increase of TNF in Tears after DS

Elevated levels of inflammatory cytokines have been described in tears of oGVHD patients [32–35]. We collected tear washings of mice from all the treatment groups and performed multiplex analysis of pro-inflammatory cytokines (IL-2, IL-4, IL-6, IL-10, TNF, IFN-γ). IL-6 and IL-10 were below the detection limit (data not shown).

There was a significantly increased TNF concentration level in tears of GVHD-DS (112 ± 83 pg/ml; p = 0.035) but not GVHD mice (53 ± 29 pg/ml; p = 0.8) compared to naïve mice (41 ± 28 pg/ml), and an increase by a trend in IFN-γ (GVHD-DS: 7.9 ± 3.5 pg/ml; p = 0.055) at d7 after BMT compared to naïve (5.0 ± 6.7 pg/ml) and GVHD (3.9 ± 4.0 pg/ml) (Fig. 4A and B). No changes were observed in the interleukins IL-2 and IL-4 (Fig. 4C and D).

These results indicate that desiccation after BMT leads to the release of pro-inflammatory cytokines into the tear film.

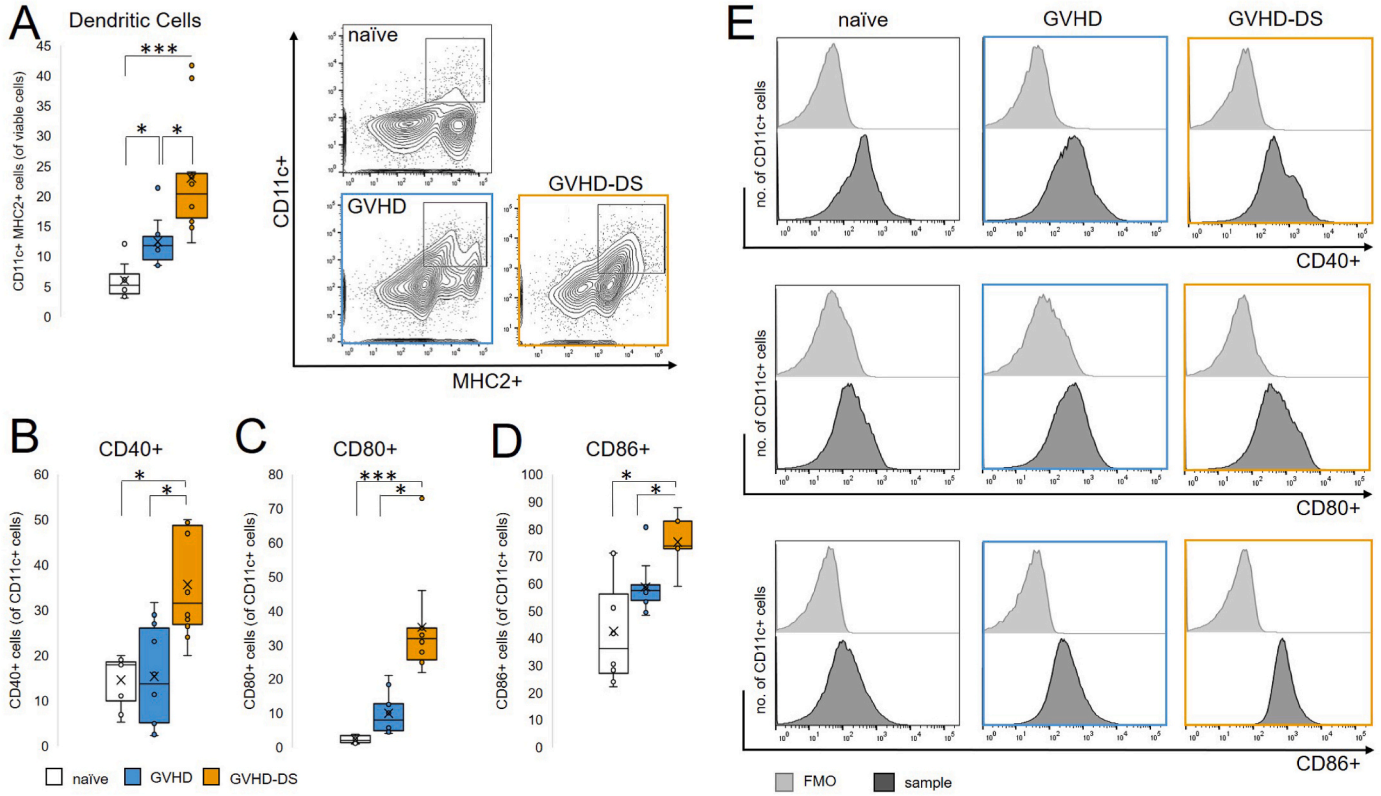

Fig. 3. Dendritic Cell (DC) analysis in cervical lymph nodes in GVHD-DS and GVHD mice at day 7 after BMT. A) The total number of $CD11c^+MHC2^+$ DCs was significantly increased in GVHD-DS compared to naïve (p = 0.04) and GVHD (p = 0.018). **B-D)** In GVHD-DS the number of $CD40^+$ (B), $CD80^+$ (C) and $CD86^+$ (D) activated DCs was significantly increased compared to GVHD mice (CD40: p = 0.006; CD80: p = 0.02; CD86: p = 0.045). In the GVHD group, the activation of DCs was comparable to naïve mice. **E)** Histograms of activation markers of DCs in representative examples of naïve, GVHD and GVHD-DS mice with FMO control that was used for gating (light grey histogram) and the antibody-treated sample (dark grey histogram). (n = 5–8 mice/group; *p ≤ 0 .05, ***p ≤ 0.0001).

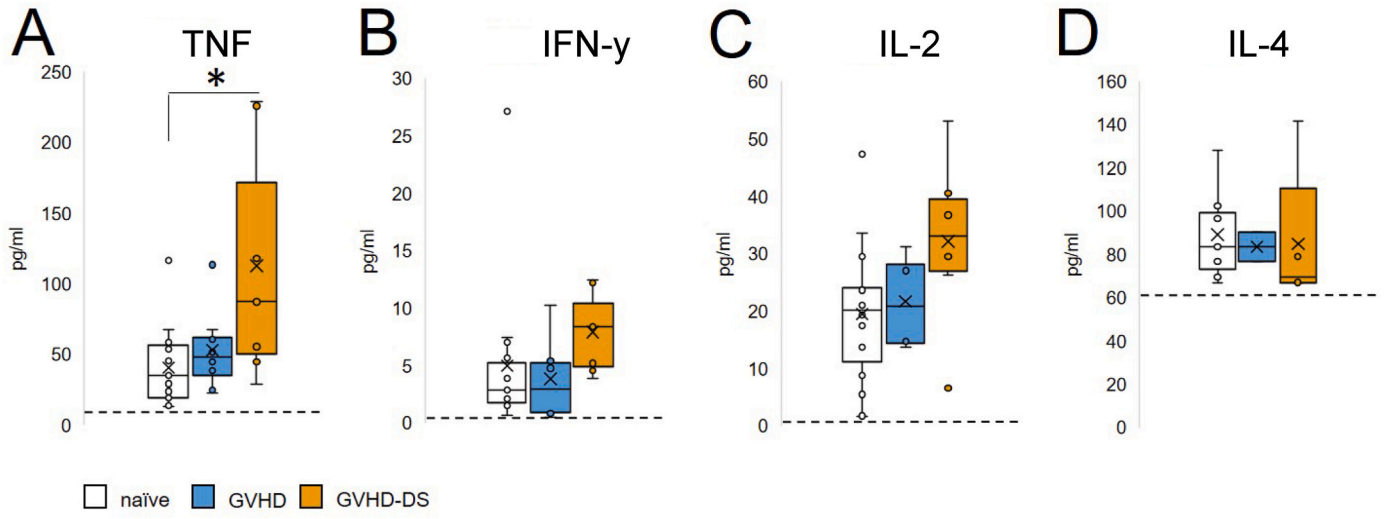

Fig. 4. Cytokine analysis in tear fluid in GVHD-DS and GVHD mice at day 7 after BMT. Tear fluid was collected as described in the methods and Luminex analysis were performed. (n = 8–10 naïve mice; n = 4–5 mice/GVHD group; 2 eyes pooled/sample; *p ≤ 0.05; dotted line = lower detection limit). **A)** TNF was significantly increased in GVHD-DS (p = 0.035) but not GVHD (p = 0.08) compared to naïve mice. **B)** IFN-γ was increased by a trend in GVHD-DS (p = 0.055), however not significantly. **C + D)** No differences were observed in the IL-2 and IL-4 concentration levels.

3.4. Differential gene expression evaluation in the cornea shows early upregulation of pro-inflammatory genes

To gain insight into the molecular pathways being differentially modulated, whole corneas were collected from all study groups, RNA was extracted, and NanoString was performed. Raw data was analyzed using ROSALIND software. A 1.5-fold change with a P-adjusted value of 0.05 was used.

First, we compared the naïve group to oGVHD with and without DS (Supplemental Fig. 1) at the day 7 timepoint. Unsupervised clustering showed that the naïve group was segregated from the two experimental groups (Supplemental Figure 1 A). Out of 594 genes in the panel, 198 genes were significantly expressed (128 down and 70 up), comparing the naïve to both experimental groups (Supplemental Fig. 1A and B). Some of these genes are depicted in the Volcano plot (Supplemental Figure 1 B). The NanoString Annotation panel showed that pathways related to "Type I″ and "Type II IFN," "MHC class I," "autoantigens" and "Th2 differentiation" were the top 5 most represented pathways (Supplemental Figure 1 C). The specific genes involved in "Type I and II IFN signaling" and "MHC class I presentation" that were differentially modulated are shown in Supplemental Figure 1 D. These results indicate that GVHD (irrespective of the presence of DS) on day 7 post-BMT causes profound changes in the cornea. As an additional analysis, we analyzed the clinical data of those two animals (one GVHD, one GVHD-DS) that did demonstrate a different gene expression pattern for "Type I Interferon" than the according group at day 7 (suppl Fig. 1 D). In these two mice, we did not see differences in the ocular phenotype, but interestingly the GVHD mouse that demonstrated similar gene expression pattern with two GVHD-DS mice had the highest systemic GVHD score of all GVHD mice. Comparatively, the GVHD-DS mouse that demonstrated a similar gene expression pattern with the two GVHD mice had the lowest systemic GVHD score of all GVHD-DS mice.

Next, we compared the naïve group to oGVHD with and without DS on day 28 post-BMT (Suppl. Fig. 2). Out of 594 genes in the panel, 310 genes were significantly expressed (108 down and 102 up), comparing the naïve to both experimental groups (Supplemental Fig. 2A and B). Some of these genes are depicted in the Volcano plot (Supplemental Figure 2 B). Similarly to the previous timepoint, the NanoString Annotation panel showed pathways related to "Type I and II IFN," "MHC I class", and "autoantigens" as part of the top 5 most represented pathways (Supplemental Fig. 2C). One difference is that "cytosolic DNA sensing" was the fourth most modulated pathway. The specific genes involved in "Type I and II IFN signaling" and "MHC class I presentation" that were differentially modulated are shown in Supplemental Figure 2 D. Some of the same genes are differentially expressed in both time points (Supplemental Figures 1 and 2 D).

We then compared GVHD to GVHD-DS. No genes passed the false discovery rate at day 7, but significantly expressed genes were observed at day 28 post-bone marrow transplant comparing GVHD-DS to GVHD (Supplemental Fig. 3). There were 75 differentially expressed genes (Supplemental Fig. 3B; 59 down and 16 up). Due to the limited number of genes, the significance score could not be calculated. Instead, we used Metascape to identify specific pathways (Supplemental Fig. 3C) that were differentially modulated. Using the 16 upregulated genes, Metascape identified that the "TGF-β pathway," "myeloid activation and regulation of metal ion transport" and "platelet activation signaling and aggregation" were the top 5 pathways in the GVHD-DS corneas (Supplemental Figure 3 C). On the other hand, Metascape analysis of the 59 downregulated genes in GVHD-DS (and by default, upregulated in the GVHD-only group) showed "positive regulation of immune response," "lymphocyte activation," "cytokine-cytokine receptor interaction," "positive regulation of cytokine production" and "TNF signaling" as the top 5 most modulated pathways (Supplemental Figure 3 D). These results indicate that GVHD-DS and GVHD activate differential immune pathways.

3.5. Increased corneal lymphangiogenesis

Based on previous findings of our group, in which corneal lymphangiogenesis is a pathomechanism of ocular GVHD [22] we hypothesize that desiccation would increase the degree of lymphangiogenesis in the cornea. To investigate this, corneas from all study groups were collected and stained with LYVE1 for lymphatics and CD31 for blood vessels. In this study, very early changes in the corneal microenvironment were observed. In the cornea of GVHD-DS animals, a significant increase in corneal lymphatics was observed already at d7 after HSCT compared to naïve controls (2.7 ± 0.4 % vs. 1.7 ± 0.6 % of total cornea; p = 0.003), but no difference was observed between GVHD (2.4 ± 1.4 % of total cornea, p = 0.065) and naïve. Also, no differences in lymph vessels were observed between GVHD-DS and GVHD (p = 0.263) (Fig. 5A and B). In contrast, corneal hemangiogenesis was not changed between the groups at d7 after HSCT (p = 0.345) (Fig. 5A–C).

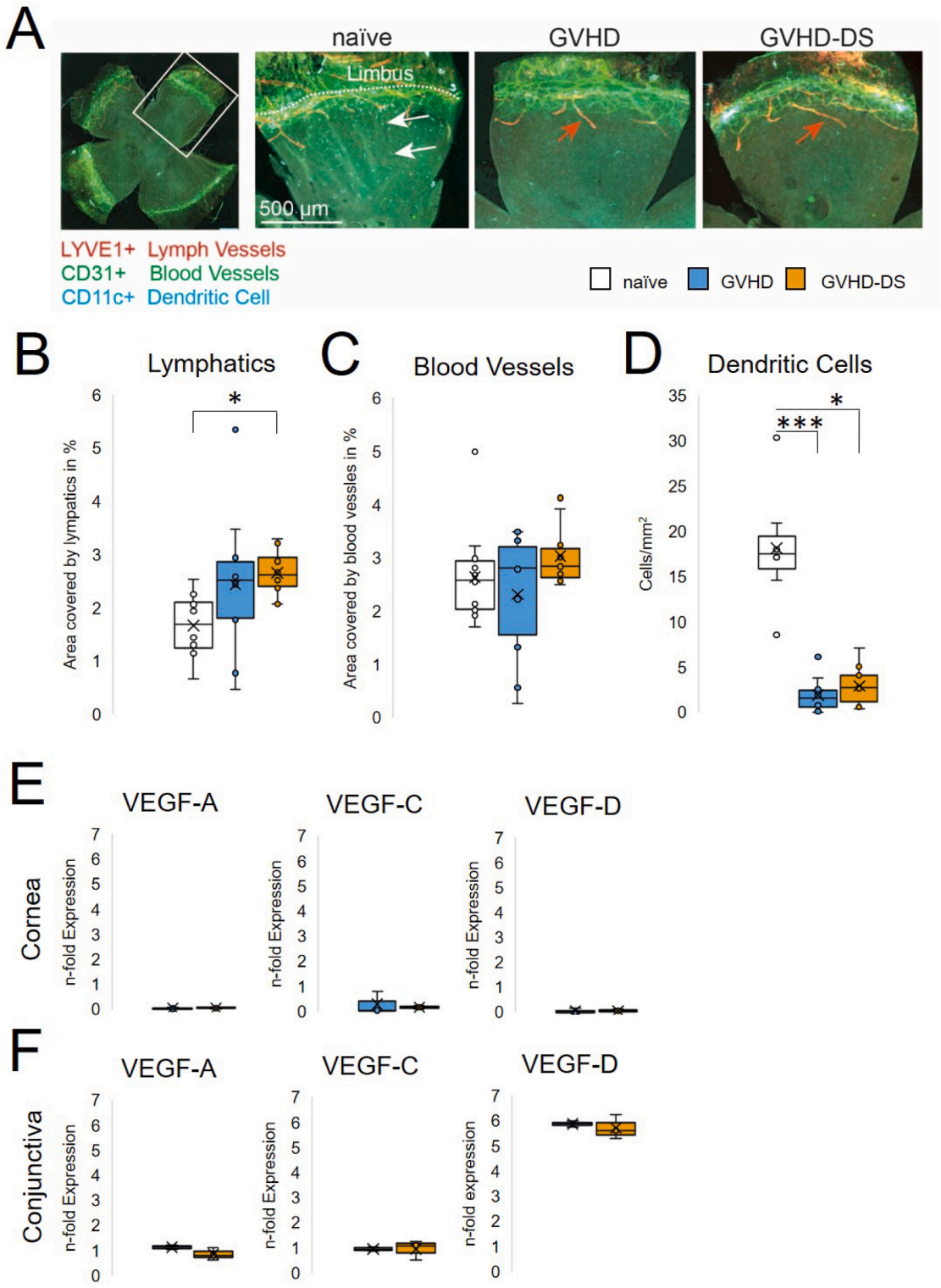

Fig. 5. Quantification of lymphatics, blood vessels and DCs in the cornea, and *vegf* expression in the cornea and conjunctiva of GVHD and GVHD-DS mice at Day 7 after BMT compared to naïve mice (immunohistochemistry, RT-qPCR). A) On the upper left an exemplarily whole mount-samples stained with CD31 (green; blood vessels), LYVE1 (red; lymphatics) and CD11c (blue; DCs). From each group one representative image was presented showing a part of the cornea from naïve, GVHD and GVHD-DS mice as indicated by the inlay on the left. At least 6 corneas were stained and analyzed/group. **B)** The total amount of corneal lymph vessels was increased in GVHD-DS ($p = 0.003$) compared to naïve mice, but not in GVHD control mice. **C)** No differences in blood vessels were observed between the groups. **D)** The number of corneal DCs was significantly decreased in both, GVHD ($p = 0.001$) and GVHD-DS ($p = 0.01$), compared to naïve control cornea. **E + F)** Expression of *vegf-a*, *-c* and *d*-in the cornea (E) and the conjunctiva (F) of GVHD (blue) and GVHD-DS (red) mice normalized to naïve controls ($n = 3$ mice/group). No differences between the groups were observed. (*$p \leq 0.05$, ***$p \leq 0.0001$. white arrow-DC; red arrow-blood vessel; VEGF-vascular endothelial growth factor). (For interpretation of the references to color in this figure legend, the reader is referred to the Web version of this article.)

In the normal cornea, there are different populations of antigen-presenting cells such as plasmacytoid and classical dendritic cells (DCs). As alterations of corneal DCs were depicted in vivo in GVHD patients and animal models [31,36,37], we investigated whether desiccating stress would lead to an increased presence of $CD11c^+$ DCs in the cornea. In GVHD-DS and GVHD, the number of $CD11c^+$ cells in the cornea was significantly reduced at d7 after BMT ($2 \pm 2/3 \pm 2$ cells/mm^2) compared to naïve cornea (18 ± 7 cells/mm^2) (GVHD: $p \leq 0.0001$; GVHD-DS: $p = 0.01$), but no differences between the groups were observed ($p = 1.0$; Fig. 5 D).

To investigate the expression of angiogenic factors, whole corneal and conjunctival tissue was analyzed regarding *vegfa*, *-c,* and *-d* mRNA transcript levels. Neither of the transcripts for these factors was different from naïve controls, and no differences were observed at d7 after HSCT (Fig. 5E and F).

In summary, these findings implicate, that desiccating stress after BMT leads to an accelerated and aggravated graft-versus-host reaction of the eye, mediated by inflammatory cytokines, adaptive immune mechanisms, and impaired immune privilege of the cornea.

4. Discussion

Recently, our group published clinical data showing that desiccating stress during the immediate post-transplant phase after aHSCT significantly increases the incidence of oGVHD [13,14]. These findings indicate that desiccating stress-related damage of the ocular surface and consecutive exposure of host antigens may lead to an early phase antigen-presentation and effector T cell responses and in humans, following time delay of months to years, reactivation of the immune response, leading to chronic oGVHD. To investigate the underlying pathomechanisms, especially in the early phase of oGVHD, we designed in-vivo experiments that best simulate this clinical situation. Our results showed that desiccating stress after BMT worsens clinical signs of ocular surface disease. Furthermore, results implicate an increase in activated $CD8^+$ cells, a decrease of FoxP3 MFI in Tregs, upregulated activation markers in dendritic cells, and increased mRNA transcript expression in the cornea of genes involved in "Type I″ and "Type II interferon" and "cytokine signaling" pathways.

Desiccating stress is a known trigger of dry eye. Clinical studies as well as the use of an experimental mouse model show that dehydration leads to epitheliopathy of the cornea and conjunctiva [23,24,26,28,38,39]. This tissue damage triggers a complex cascade involving both innate and acquired immune mechanisms. In dry eye, increased levels of pro-inflammatory molecules such as TNF and IFN-γ are found in the tear film and increased activation of corneal dendritic cells [40,41]. This can also be visualized in vivo in patients using confocal microscopy [31,42]. After the expansion of autoreactive T cells, homing to the ocular surface and chronic Th17 T cell-mediated inflammation occurs [43]. In desiccating stress-induced dry eye, there are some parallels to the results presented here concerning the induction of a mucosal immune response.

Experimental analysis of the pathogenesis of oGVHD has so far focused on late changes such as destruction and fibrosis of the ocular surface and lacrimal gland [15,16,20,21,44]. Very early changes have not yet been investigated in detail, especially not under adverse environmental conditions.

Apart from an expected early activation of the innate immune system, which is also crucial in the first phase of the development of non-ocular chronic GVHD [4], T cells and DCs play a central role in the early development of GVHD after desiccation stress. However, whether these are primarily recipient-derived cells or donor cells that migrated early into the cornea is unclear. Previous experiments by Heretes et al. on the migration of immune cells into the cornea show that a population of donor-derived $CD4^+$ and $CD8^+$ T cells in the cornea appear as early as 2–3 weeks after transplantation [18].

Investigating $CD4^+$ and $CD8^+$ T cells in cervical lymph nodes in the present study, a higher number of $CD8^+$ T cells were detected in both GVHD and GVHD-DS groups in comparison to naïve mice. However, no statistical difference was present between the GVHD groups. To investigate the activation of $CD8^+$ T cells, we analyzed the co-expression of CD25. In both GVHD groups an increased frequency of activated $CD8^+CD25^+$ T cells were detected, implicating an early initiation of an effector response. Although our studies did not find a decrease in the frequency of $CD4^+CD25^+FoxP3^+$ in ocular draining nodes, the MFI of $FoxP3^+$ was significantly decreased in the GVHD-DS group. FoxP3 is critical for the maintenance of Treg function, as mice deficient in FoxP3 develop severe autoimmunity [45,46]. These findings suggest that Treg's suppressive ability in the GVHD-DS group could be decreased. The indication of functionally ineffective Tregs fits with previous evidence that loss of function of $FoxP3^+$ Tregs plays a central role in various autoimmune diseases including GVHD [47]. Furthermore, Tregs are central mediators of immune tolerance after aHSCT. Reduced function of Tregs, on the other hand, leads to an amplification of GVHD and is subject to T cell-based microRNA-31/hypoxia-inducible factor 1a regulation [48].

Dendritic cells were not examined in previous mouse experiments but in clinical studies using confocal laser scanning microscopy of the cornea of patients with chronic oGVHD [31,36]. Here, an increased density of DCs was found in the central and peripheral cornea, although recent evidence was published stating that some of these cells may be activated T-cells [49]. In addition, these studies were performed months to years after transplantation, and it is not possible to differentiate between donor and recipient-derived cells with this technique. For this reason, further experimental studies are warranted to test the hypothesis that donor-derived dendritic cells initiate an early adaptive immune response to desiccation stress.

In our study, the number of DCs in cervical lymph nodes was significantly increased in GVHD-DS mice 7 days after transplantation furthermore demonstrating a significant activation by expressing co-stimulatory molecules CD40, CD80, and CD86. In the non-desiccated group, although increased by number, no increase of activated dendritic cells in comparison to naïve mice was observed, implicating, that desiccating stress triggers not only an increase of DCs in cervical lymph nodes but also DC activation as early as day 7 after transplantation.

Tear cytokines have been investigated in several human studies as potential biomarkers for oGVHD (overview in Ref. [50]). It has been shown that IL- 2, -6, -8, -10, −17, and IFN-γ, as well as TNF, are increased in chronic oGVHD [34,51], while endothelial growth factor (EGF) is decreased [32,33]. Compared to age- and sex-matched healthy controls, IFN-γ was particularly elevated in the early stages of oGVHD, while elevated IL-6 levels were correlated with oGVHD in later stages [51]. In addition, IL-6, IL-8, IL-10, and TNF have been reported to correlate with the severity of oGVHD as measured by corneal fluorescein staining and tear film break-up time [33]. Higher IFN-γ concentrations in tear fluid were also detected in an autoimmune Sjögren's disease-like dry eye mouse model during age-related inflammation and showed a correlation between IFN-γ and disease severity [52]. In another inducible dry eye mouse model, increased TNF levels were described in tear samples from individual animals compared to naïve mice [53]. The analyses performed in our study show a significant increase in TNF and (trend towards) an increase in IFN-γ in comparison to naïve mice at a very early time point, which matches the results published from humans and indicates a general early onset inflammatory response at the ocular surface.

Gene expression demonstrated a profound difference between naïve and GVHD/GVHD-DS mice. Further analysis showed, that at both time points (d7 and d28) "Type I and II Interferon" as well as "MHC I pathways" were most expressed (Suppl. Figs. 1 and 2). However, a more detailed analysis of gene regulation related to these pathways did not allow precise clustering within the groups. Analyzing gene expression between GVHD and GVHD-DS at d28 furthermore demonstrated that desiccation during aHSCT and engraftment leads to activation of pathways such as "TGF-β"," myeloid cell activation," "regulation of metal ion

transport" and "response to fungus" (Suppl. Fig. 3). Instead, non-desiccation GVHD leads to activation of pathways including "lymphocyte activation," "cytokine-production" and "TNF signaling." These results are a first hint that different immune pathways are activated depending on whether ocular surface desiccation is present during aHSCT. If confirmed in larger sampled studies including human tissue samples, this could lead to profoundly different prophylactic strategies using different immunosuppressive agents.

A major difference to dry eye disease is the early lymphangiogenesis during oGVHD. This is not seen reproducibly in desiccating stress-induced dry eye, only with the additional experimental increase of local tissue destruction or inflammation [54]. Corneal lymphangiogenesis in ocular GVHD could serve as evidence of increased severity or activity, which is also reflected in the clinical comparison between dry eye and chronic ocular GVHD [2,54]. Comparing GVHD mice to naïve mice in a previous study, we detected corneal lymphangiogenesis as early as day 14 [22]. Following desiccating stress, however, corneal lymphangiogenesis is already present at day 7, correlating well with the clinically significant increase of oGVHD severity in these experiments.

In our animal model, the greatly increased immune response affects not only the eyes but the entire organism. A significantly increased systemic GVHD score reflects this and should be the starting point for further studies. Interestingly, patients transplanted under stress do not show increased GVHD scores in other organs, especially the skin, compared to patients transplanted under normal humidity [13].

Based on the data presented here, we postulate the following pathogenesis of desiccating stress-triggered oGVHD (Fig. 6): In the non-desiccated environment at early time points, conjunctival epithelium is intact, non-activated donor-derived DCs are present together with a low number of Tregs that can regulate migrating effector cells $CD4^+$ and $CD8^+$ (Fig. 6A). In contrast, desiccation causes epithelial damage to the ocular surface, leading to consecutive increases in gene signaling and the release of pro-inflammatory factors related to innate immunity. Activated dendritic cells emigrate through conjunctival and newly formed corneal lymphatic vessels, followed by expansion of effector T-cells. Furthermore, impaired Tregs are incapable of reducing the accelerated local immune response (Fig. 6B).

Regarding the translation of the data, there are several limitations related to the not fully understood immunopathogenesis, the high individuality of patients, and the chosen animal model: Further experimental and clinical studies must confirm which immunopathological alterations occur after dehydration stress. Therapeutic targets should be identified and tested with appropriate substances. In contrast to patients, none of the established oGVHD models take into account the pre-existence of a blood cancer disease or include mice with this disease. Therefore, blood cancer-associated factors might play a role in humans that have not been considered in the experiments performed so far. Finally, in the animal model, all mice develop GVHD and not 40–60 % as in humans [22]. Thus, mechanisms or factors that prevent oGVHD in patients despite desiccating stress cannot be simulated in animal models, although they are of great clinical interest. Statistical comparisons between GVHD and GVHD-DS did not show significant differences in several analyses. However, comparing each group with naïve animals (resembling a baseline situation before bone marrow transplantation) demonstrated significant changes in relevant immunopathological processes at very early time points. By increasing sample sizes in follow-up experiments we believe, that significance levels will also be achieved in the group by group comparison.

In summary, our experiments show that desiccating stress during experimental aHSCT leads to a pronounced increase in oGVHD severity. These data confirm our previous data from retrospective clinical studies in which patients under desiccation stress develop oGVHD to a significantly higher degree than patients transplanted under normal humidity conditions [13,14]. The prevention of ocular surface desiccation and the development of prophylactic-specific immunomodulatory therapies applied before or at very early time points after aHSCT have the potential to reduce the proportion of patients with oGVHD.

Data repository

The data published here can be freely accessed at https://osf.io/ewgyx/?view_only=60842589bfe14ce782aaec4f61131d69.

Funding support

This work was supported by Deutsche Forschungsgemeinschaft Research Unit FOR2240 (DFG STE1928/7-1, DFG GE3108/101), SFB1607 (project B01). CSdP receives salary support from the Caroline Elles Professorship and from an unrestricted grant from Research to Prevent Blindness.

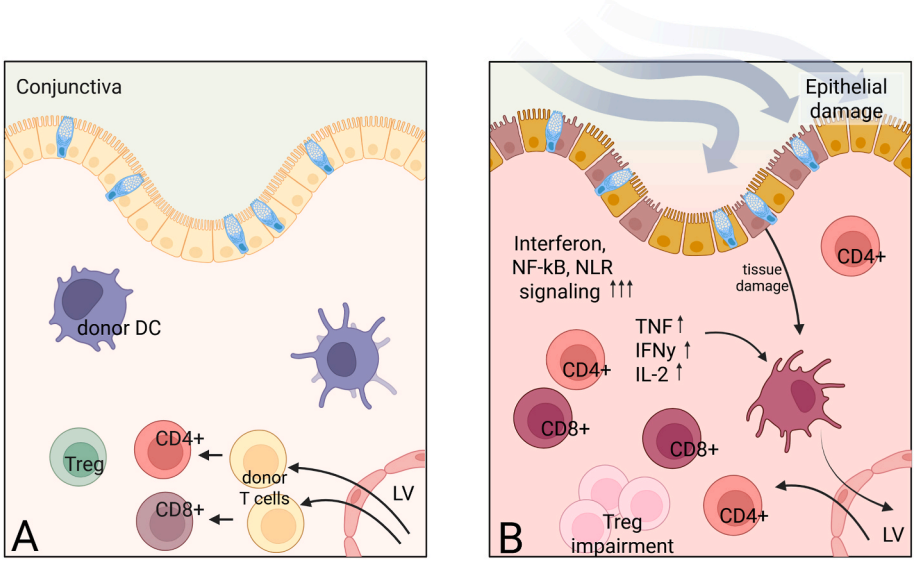

Fig. 6. Proposed pathomechanisms of early phase ocular GVHD following desiccating-stress. A: non-desiccated environment. B: desiccated environment (LV: lymphatic vessel, image created with BioRender, https://BioRender.com/6br7yzm).

CRediT authorship contribution statement

Uta Gehlsen: Writing – original draft, Visualization, Methodology, Formal analysis. **Martina Maass:** Writing – original draft, Visualization, Investigation, Formal analysis. **Daniela Stary:** Investigation. **Svenja Wagener-Ryczek:** Methodology. **Gwen Musial:** Software. **Manolis Pasparakis:** Writing – review & editing. **Cintia S. de Paiva:** Writing – original draft, Visualization, Formal analysis. **Michael E. Stern:** Writing – original draft, Conceptualization. **Philipp Steven:** Writing – original draft, Supervision, Resources, Methodology, Investigation, Formal analysis, Conceptualization.

Acknowledgments

The authors would like to thank Timur Bilgin and Anna-Lena Zachert for their excellent animal work and their extraordinary technical performance. We are grateful to Dr. Anne Kiesewetter for her support with the tear film cytokine analysis.

Appendix A. Supplementary data

Supplementary data to this article can be found online at https://doi.org/10.1016/j.jtos.2025.04.008.

Abbreviations

AB	antibody
CD	cluster of differentiation
DC	dendritic cell
DEG	differentially expressed gene
DS	desiccating stress (=reduced humidity and airflow)
EGF	endothelial growth factor
FoxP3	forkhead box P3 protein
GSS	global significance score
(o)GVHD	(ocular) graft-versus-host-disease
HSCT	hematopoietic stem cell transplantation
ICAM1	intercellular adhesion molecule 1
IL	interleukin
IVCM	in vivo confocal microscopy
KC/CXCL1	keratinocyte-derived chemokine/chemokine (C-X-C) ligand 1
LIX/CXCL5	epithelial-derived neutrophil-activating peptide/ chemokine (C-X-C) ligand 5
MFI	mean fluorescence intensity
MIP-2/CXCL2	macrophage inflammatory protein 2/chemokine (C-X-C) ligand 2
rH	room humidity
VEGF	vascular endothelial growth factor

References

[1] Wolff D, et al. National institutes of health consensus development project on criteria for clinical trials in chronic graft-versus-host disease: IV. The 2020 highly morbid forms report. Transplant Cell Ther 2021;27(10):817–35.
[2] Kitko CL, et al. National institutes of health consensus development project on criteria for clinical trials in chronic graft-versus-host disease: IIa. The 2020 clinical implementation and early diagnosis working group report. Transplant Cell Ther 2021;27(7):545–57.
[3] Mirza N, et al. Graft versus self (GvS) against T-cell autoantigens is a mechanism of graft-host interaction. Proc Natl Acad Sci U S A 2016;113(48):13827–32.
[4] Zeiser R, Blazar BR. Pathophysiology of chronic graft-versus-host disease and therapeutic targets. N Engl J Med 2017;377(26):2565–79.
[5] Wilhelm K, et al. Graft-versus-host disease is enhanced by extracellular ATP activating P2X7R. Nat Med 2010;16(12):1434–8.
[6] Flynn R, et al. Increased T follicular helper cells and germinal center B cells are required for cGVHD and bronchiolitis obliterans. Blood 2014;123(25):3988–98.
[7] Dertschnig S, et al. Impaired thymic expression of tissue-restricted antigens licenses the de novo generation of autoreactive CD4+ T cells in acute GVHD. Blood 2015;125(17):2720–3.
[8] Zeiser R, et al. Danger signals activating innate immunity in graft-versus-host disease. J Mol Med (Berl) 2011;89(9):833–45.
[9] Soleimani M, et al. Ocular graft-versus-host disease (oGVHD): from A to Z. Surv Ophthalmol 2023;68(4):697–712.
[10] Malta JB, et al. Treatment of ocular graft-versus-host disease with topical cyclosporine 0.05%. Cornea 2010;29(12):1392–6.
[11] Cantu-Rodriguez OG, et al. Cyclosporine A for the prevention of ocular graft versus host disease in allogeneic hematopoietic stem cell transplant recipients is safe and feasible. Acta Haematol 2020;143(5):425–31.
[12] Chun YH, et al. Topical cyclosporine pretreatment of ocular surface in allogeneic hematopoietic stem cell transplant recipients. J Ocul Pharmacol Therapeut 2018;34(9):628–32.
[13] Gehlsen U, et al. Desiccating stress significantly increases the risk for chronic ocular graft-versus-host-disease. Transplant Cell Ther 2022;28(11). p. 782 e1-782 e7.
[14] Steven P, et al. Adverse environmental conditions are a risk factor for ocular GvHD after allogeneic hematopoietic stem cell transplantation. Bone Marrow Transplant 2020;55(9):1851–3.
[15] Perez VL, et al. Meibomian gland dysfunction: a route of ocular graft-versus-host disease progression that drives a vicious cycle of ocular surface inflammatory damage. Am J Ophthalmol 2022;247:42–60.
[16] Perez RL, et al. Limbus damage in ocular graft-versus-host disease. Biol Blood Marrow Transplant 2011;17(2):270–3.
[17] Levy RB, et al. Analyses and correlation of pathology and ocular cutaneous changes in murine graft versus host disease. Int J Mol Sci 2021;23(1).
[18] Herretes S, et al. Recruitment of donor T cells to the eyes during ocular GVHD in recipients of MHC-matched allogeneic hematopoietic stem cell transplants. Investig Ophthalmol Vis Sci 2015;56(4):2348–57.
[19] Yang F, et al. Eyelid blood vessel and meibomian gland changes in a sclerodermatous chronic GVHD mouse model. Ocul Surf 2022;26:328–41.
[20] Yamane M, et al. Senescence-associated secretory phenotype promotes chronic ocular graft-vs-host disease in mice and humans. FASEB J 2020;34(8):10778–800.
[21] Yaguchi S, et al. Angiotensin II type 1 receptor antagonist attenuates lacrimal gland, lung, and liver fibrosis in a murine model of chronic graft-versus-host disease. PLoS One 2013;8(6):e64724.
[22] Gehlsen U, et al. Ocular graft-versus-host disease in a chemotherapy-based minor-mismatch mouse model features corneal (lymph-) angiogenesis. Int J Mol Sci 2021;22(12).
[23] Dursun D, et al. A mouse model of keratoconjunctivitis sicca. Investig Ophthalmol Vis Sci 2002;43(3):632–8.
[24] Gehlsen U, et al. A semifluorinated alkane (F4H5) as novel carrier for cyclosporine A: a promising therapeutic and prophylactic option for topical treatment of dry eye. Graefes Arch Clin Exp Ophthalmol 2017;255(4):767–75.
[25] Riesner K, et al. A preclinical acute GVHD mouse model based on chemotherapy conditioning and MHC-matched transplantation. Bone Marrow Transplant 2016;51(3):410–7.
[26] De Paiva CS, et al. IL-17 disrupts corneal barrier following desiccating stress. Mucosal Immunol 2009;2(3):243–53.
[27] Lopez-Miguel A, et al. Dry eye exacerbation in patients exposed to desiccating stress under controlled environmental conditions. Am J Ophthalmol 2014;157(4):788–98. pp. e2.
[28] Niederkorn JY, et al. Desiccating stress induces T cell-mediated Sjogren's Syndrome-like lacrimal keratoconjunctivitis. J Immunol 2006;176(7):3950–7.
[29] Kulkarni MM. Digital multiplexed gene expression analysis using the NanoString nCounter system. Curr Protoc Mol Biol 2011. https://doi.org/10.1002/0471142727.mb25b10s94.
[30] Rojas B, et al. Cell populations and adhesion molecules expression in conjunctiva before and after bone marrow transplantation. Exp Eye Res 2005;81(3):313–25.
[31] He J, et al. In vivo confocal microscopy evaluation of ocular surface with graft-versus-host disease-related dry eye disease. Sci Rep 2017;7(1):10720.
[32] Cocho L, et al. Biomarkers in ocular chronic graft versus host disease: tear cytokine- and chemokine-based predictive model. Investig Ophthalmol Vis Sci 2016;57(2):746–58.
[33] Hu B, Qiu Y, Hong J. Tear cytokine levels in the diagnosis and severity assessment of ocular chronic graft-versus-host disease(GVHD). Ocul Surf 2020;18(2):298–304.
[34] Jung JW, et al. Tear cytokines as biomarkers for chronic graft-versus-host disease. Biol Blood Marrow Transplant 2015;21(12):2079–85.
[35] Nair S, et al. Tear inflammatory mediators and protein in eyes of post allogenic hematopoeitic stem cell transplant patients. Ocul Surf 2018;16(3):352–67.
[36] Steger B, et al. In vivo confocal microscopic characterisation of the cornea in chronic graft-versus-host disease related severe dry eye disease. Br J Ophthalmol 2015;99(2):160–5.
[37] Yu H, et al. Dendritic cell regulation of graft-vs.-host disease: immunostimulation and tolerance. Front Immunol 2019;10:93.
[38] De Paiva CS, et al. Dry eye-induced conjunctival epithelial squamous metaplasia is modulated by interferon-gamma. Investig Ophthalmol Vis Sci 2007;48(6):2553–60.
[39] Yeh S, et al. Apoptosis of ocular surface cells in experimentally induced dry eye. Investig Ophthalmol Vis Sci 2003;44(1):124–9.
[40] Lee HS, Amouzegar A, Dana R. Kinetics of corneal antigen presenting cells in experimental dry eye disease. BMJ Open Ophthalmol 2017;1(1):e000078.
[41] Maruoka S, Inaba M, Ogata N. Activation of dendritic cells in dry eye mouse model. Investig Ophthalmol Vis Sci 2018;59(8):3269–77.
[42] Kheirkhah A, et al. Corneal epithelial immune dendritic cell alterations in subtypes of dry eye disease: a pilot in vivo confocal microscopic study. Investig Ophthalmol Vis Sci 2015;56(12):7179–85.

[43] Stern ME, et al. Autoimmunity at the ocular surface: pathogenesis and regulation. Mucosal Immunol 2010;3(5):425–42.
[44] Ogawa Y, et al. Immune processes and pathogenic fibrosis in ocular chronic graft-versus-host disease and clinical manifestations after allogeneic hematopoietic stem cell transplantation. Cornea 2010;29(Suppl 1):S68–77.
[45] Freuchet A, et al. IL-34 deficiency impairs FOXP3(+) Treg function in a model of autoimmune colitis and decreases immune tolerance homeostasis. Clin Transl Med 2022;12(8):e988.
[46] Zemmour D, et al. Single-cell analysis of FOXP3 deficiencies in humans and mice unmasks intrinsic and extrinsic CD4(+) T cell perturbations. Nat Immunol 2021;22(5):607–19.
[47] Mancusi A, et al. CD4(+)FOXP3(+) regulatory T cell therapies in HLA haploidentical hematopoietic transplantation. Front Immunol 2019;10:2901.
[48] Wu Y, et al. MicroRNA-31 regulates T-cell metabolism via HIF1alpha and promotes chronic GVHD pathogenesis in mice. Blood Adv 2022;6(10):3036–52.
[49] Downie LE, et al. Redefining the human corneal immune compartment using dynamic intravital imaging. Proc Natl Acad Sci U S A 2023;120(31). p. e2217795120.
[50] Crossland RE, et al. Potential novel biomarkers in chronic graft-versus-host disease. Front Immunol 2020;11:602547.
[51] Riemens A, et al. Cytokines in tear fluid of patients with ocular graft-versus-host disease after allogeneic stem cell transplantation. Mol Vis 2012;18:797–802.
[52] De Paiva CS, et al. Age-related T-cell cytokine profile parallels corneal disease severity in Sjogren's syndrome-like keratoconjunctivitis sicca in CD25KO mice. Rheumatology 2010;49(2):246–58.
[53] Contreras-Ruiz L, et al. A nanomedicine to treat ocular surface inflammation: performance on an experimental dry eye murine model. Gene Ther 2013;20(5):467–77.
[54] Clahsen T, et al. The novel role of lymphatic vessels in the pathogenesis of ocular diseases. Prog Retin Eye Res 2023;96:101157.